

# Response of DIMM turbulence sensor

A. Tokovinin

Version 1. December 20, 2006 [tdimm/doc/dimmsensor.tex]

## 1 Introduction

Differential Image Motion Monitor (DIMM) is an instrument destined to measure optical turbulence (seeing or  $r_0$ ) from the variance of the longitudinal and transverse image motion between two apertures. Generally, the apertures are circular of diameter  $D$  separated by the baseline  $B$ .

The standard DIMM theory provides the response coefficient  $K$  relating the variance of differential image motion  $\sigma_\alpha^2$  to  $r_0$ ,

$$\sigma_\alpha^2 = K(\lambda/D)^2(D/r_0)^{5/3}. \quad (1)$$

In fact, the combination on the right-hand side is independent of  $\lambda$ , so, in theory, DIMM is completely achromatic. The coefficients  $K_l$  and  $K_t$  for longitudinal and transverse motion are usually calculated by assuming Kolmogorov turbulence model. In theory,  $\alpha$  is the true centroid (or average wave-front gradient, also called G-tilt).

In reality, the positions of spots are calculated by some centroiding method which is only an approximation for the true centroid. The number of image pixels in centroid calculation has to be restricted in order to reduce the influence of the detector noise. The relation between the *signal*  $s$  and true centroid is not simple. It is complicated even more when optical aberrations and propagation effects are considered.

**The purpose of this study is to evaluate the influence of centroid methods, optical aberrations, and propagation on the DIMM response coefficients  $K$ .** An analytical method for calculating small-signal response  $K$  is developed and verified by numerical simulations.

## 2 Main relations

The centroid signal  $s$  for each spot is obtained from the weighted PSF  $I(\mathbf{a})$  as

$$s = I_0^{-1} \int I(\mathbf{a}) W(\mathbf{a}) d^2\mathbf{a}, \quad (2)$$

where  $\mathbf{a}$  is a 2-dimensional vector of angular coordinates,  $W(\mathbf{a})$  is the *weight* or mask, and  $I_0$  is the total intensity (flux), possibly including some weighting. All integrals are in infinite limits and exist because all functions are supposed to have limited support. The PSF is not necessarily an ideal one, but may include some aberrations. The mask  $W(\mathbf{a})$  is chosen so that the signal  $s$  is proportional to the spot centroid.

Let  $\mathbf{x}$  be the coordinate vector in the pupil plane (in meters). The complex amplitude of the initial un-perturbed field at the pupil is  $U(\mathbf{x})$ . It includes the pupil function (possibly with aberrations) and is normalized arbitrarily.

Suppose that the amplitude  $U$  is changed by a small phase aberration  $\varphi(\mathbf{x})$  and a small log-amplitude perturbation  $\chi(\mathbf{x})$  and becomes  $U(\mathbf{x}) e^{i\varphi(\mathbf{x})+\chi(\mathbf{x})}$ . What would be the change of the signal  $\Delta s$  caused by this aberration? The analysis [not given here] leads to the expressions

$$\Delta s_\varphi = \int F_\varphi(\mathbf{x}) \varphi(\mathbf{x}) d^2\mathbf{x}, \quad \Delta s_\chi = \int F_\chi(\mathbf{x}) \chi(\mathbf{x}) d^2\mathbf{x}, \quad (3)$$

where the *filter functions*  $F$  are

$$F_\varphi(\mathbf{x}) = -\text{Im}[A(\mathbf{x})], \quad F_\chi(\mathbf{x}) = \text{Re}[A(\mathbf{x})] \quad (4)$$

and

$$A(\mathbf{x}) = 2 (\lambda I_0)^{-1} U(\mathbf{x}) \int U^*(\mathbf{x} + \mathbf{x}') \tilde{W}(\mathbf{x}'/\lambda) d^2\mathbf{x}' = I_0^{-1} U [U^* \star \tilde{W}]. \quad (5)$$

In the symbolic notation  $\star$  denotes correlation and the argument scaling of  $\tilde{W}$  (Fourier transform of  $W$ ) is omitted. Clearly, the response is independent of the normalization of the amplitude  $U$  because it is divided by the flux.

This result contains an implicit assumption that the fluctuations of the denominator  $I_0$  can be neglected. This is not always true. The signal has the form  $s = A/B$ , hence its fluctuations are  $\Delta s = \Delta A/B - s \times (\Delta B/B)$ . The fluctuations of the denominator  $\Delta B$  can be neglected if the average signal  $s = 0$  (they will be a second-order term then). This condition is enforced by the choice of the mask.

### 3 Centroid methods

Calculation of the centroid in x-direction is done with the mask

$$W_x(\mathbf{a}) = (a_x - a_0) W_0(a). \quad (6)$$

Here  $a = |\mathbf{a}|$  is the radial distance from the image center,  $a_x$  is the angular coordinate along x-axis.  $W_0(a)$  is a function selecting relevant pixels and  $a_0$  is a constant that ensures zero average signal. It is easily shown that  $a_0 = I_0^{-1} \int a_x I W_0 d^2\mathbf{a}$ . The exact value of the constant  $a_0$  is not important because it adds only a constant (non-fluctuating) part to the signal  $s$ . The total intensity is computed with the same weight,

$$I_0 = \int I(\mathbf{a}) W_0(\mathbf{a}) d^2\mathbf{a}. \quad (7)$$

There are several possible choices of the weight  $W_0$ , for example:

1. *Circular window* with radius  $\rho$ :  $W_0$  is equal to one for  $a < \rho$  and zero elsewhere. This is the default choice studied here.
2. *Thresholding*:  $W_0$  is equal to one for pixels with  $I \geq T \times I_{max}$ , where  $T$  is the relative threshold.

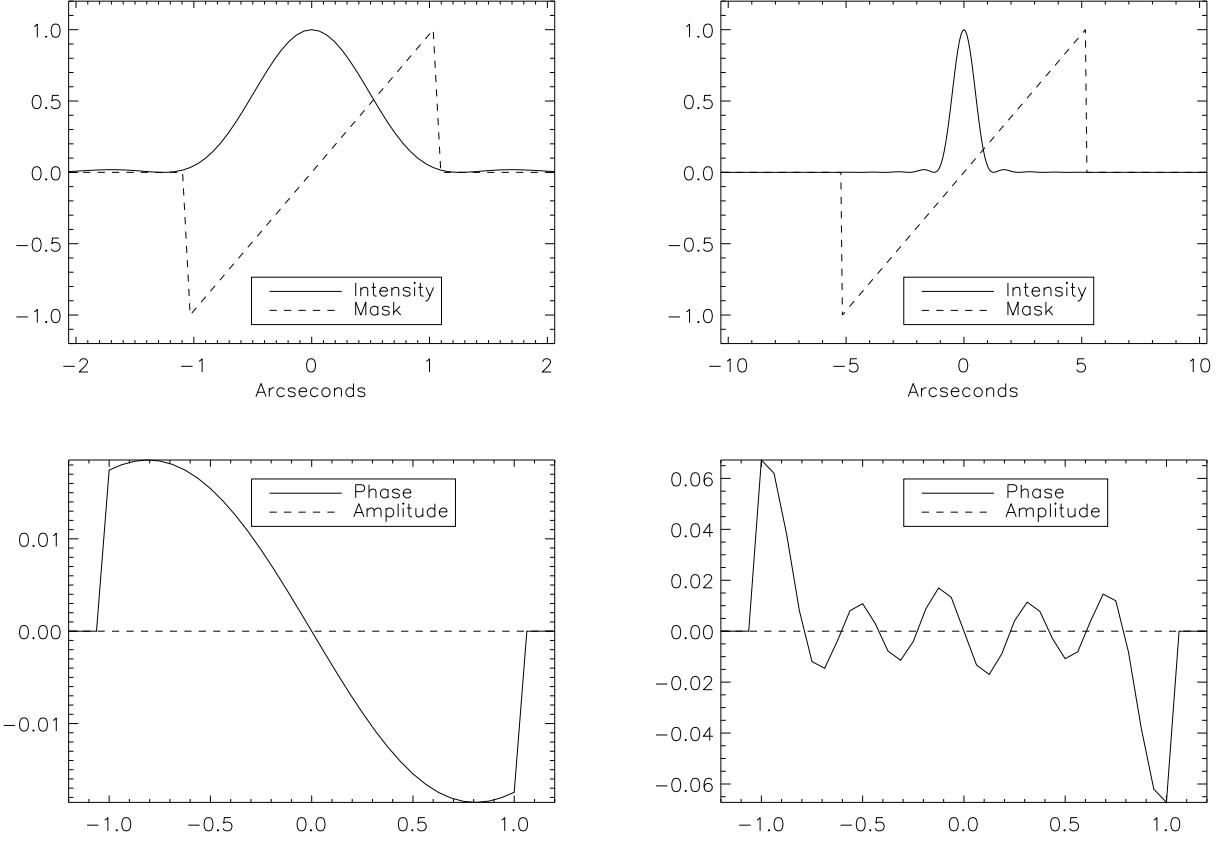


Figure 1: The masks and image profiles (top row) and corresponding phase and amplitude responses (bottom row) for a narrow mask  $\delta = 1$  (left) and a wide mask  $\delta = 5$  (right). No aberrations.

In the following, the mask radius  $\rho$  is expressed as a fraction  $\delta$  of the diffraction radius of the spot,  $\rho = \delta \times \lambda/D$ .

Figure 1 shows the influence of the mask's width on the response to phase perturbations calculated for  $D = 0.1$  m and  $\lambda = 0.5 \mu\text{m}$ . For a narrow mask, the response  $F_\varphi$  resembles roughly a Zernike tilt. On the other hand, the response of a centroid calculated in a wide window resembles two opposite-sign delta-functions at the pupil borders, i.e. is closer to the true average gradient (G-tilt). The amplitude response  $F_\chi$  is zero. However, this will not be the case for aberrated spots (see below).

## 4 Response coefficients

Here we calculate the variance of the signal  $s$  caused by a weak atmospheric turbulence. The basis of this derivation has been given by Noll [1]. The Kolmogorov model gives the atmospheric phase spatial spectrum as

$$\Phi_\varphi(f) = 0.0229 r_0^{-5/3} f^{-11/3} \quad (8)$$

(cf. Roddier [2]), where  $\mathbf{f}$  is the spatial-frequency vector,  $f = |\mathbf{f}|$ . Using the Wiener-Khinchin theorem and the relation between  $s$  and phase (3), the signal variance becomes

$$\sigma_s^2 = \int |\tilde{F}_\varphi(\mathbf{f})|^2 \Phi_\varphi(\mathbf{f}) d^2\mathbf{f}. \quad (9)$$

If the weight  $W$  is correctly dimensioned to compute the signal  $s$  in pixels and the angular size of the pixel is  $p$ , then it follows that the response coefficient for the single spot motion can be computed as

$$K = (pD/\lambda)^2 (r_0/D)^{5/3} \int |\tilde{F}_\varphi(\mathbf{f})|^2 \Phi_\varphi(\mathbf{f}) d^2\mathbf{f}. \quad (10)$$

For the differential motion, the additional filter  $M^2(\mathbf{f}) = [2 \sin(\pi B f_x)]^2$  has to be inserted under the integral (10). This filter corresponds to the difference of phases over a baseline  $B$ , assumed here to parallel to the x-axis.

The response coefficients for pure G-tilts have been calculated analytically (cf. discussion and references in [3]) and can be approximated as

$$\begin{aligned} K_l &= 0.340 (1. - 0.570b^{-1/3} - 0.04b^{-7/3}) \\ K_t &= 0.340 (1. - 0.855b^{-1/3} + 0.03b^{-7/3}). \end{aligned} \quad (11)$$

**Propagation effects.** The above calculation of the response coefficient is valid only for a near-field, pure phase turbulence. After propagation by some distance  $z$ , part of the phase fluctuations is converted to the amplitude fluctuations. In the Fourier domain, the phase is multiplied by the spatial filter  $\cos(\pi\lambda z f^2)$ , and the amplitude is obtained from the phase by the filter  $\sin(\pi\lambda z f^2)$ . Combining phase and amplitude with the corresponding filters  $\tilde{F}_\varphi$  and  $\tilde{F}_\chi$ , we can show that for calculating a response of the sensor to a turbulent layer at a distance  $z$ , we can still use Eq. 10 with a modified filter,

$$|\tilde{F}_\varphi(\mathbf{f})|^2 \rightarrow |\tilde{F}_\varphi(\mathbf{f}) \cos(\pi\lambda z f^2) - \tilde{F}_\chi(\mathbf{f}) \sin(\pi\lambda z f^2)|^2. \quad (12)$$

This modification automatically accounts for the correlation between phase and amplitude (i.e. scintillation) effects. The cross-spectrum of phase and amplitude fluctuations is not zero (the statement to the contrary on p. 332 of [2] is wrong). Phase and amplitude are un-correlated at any point because the *integral* of the cross-spectrum is zero, but the general covariance function  $\langle \varphi\chi \rangle$  is not zero everywhere. If the cross-spectrum is neglected, the resulting propagation-dependent response coefficient becomes wrong.

Summarizing, the analytic calculation of the response is done in several steps. First, define the optical system (hence amplitude  $U$ ) and the centroid method (mask  $W_x$  for longitudinal or  $W_y$  for transverse motion). Second, compute the response functions  $F_\varphi$  and  $F_\chi$  using (4,5). If the propagation distance is not zero, get the modified filter according to (12). Finally, compute the response  $K$  from (10).

## 5 Numeric calculation of the response and its validation

The analytic calculation of the response coefficients for DIMM is implemented in the IDL code `respdimm.pro`. The integrals are computed as finite sums of 2D square arrays. The number of

grid points in these arrays is chosen sufficiently large, typically  $2 N_{grid} = 512$ . Much larger grids lead to prohibitively long calculation and the accumulation of round-off errors.

Accurate analytical calculation of the response is non-trivial. The parameter  $K_{size} = L/D$  defines the ratio of the grid size to the aperture diameter. If it is just above one, the aperture is well modeled, but the PSF calculated by the FFT will be severely under-sampled, as well as the mask. A compromise  $K_{size} = 16$  works well, with 8 and 32 also acceptable choices. The next problem is the integration of the power spectrum represented by Eq. 10. The integral is well behaved near zero frequency because the  $f^{-11/3}$  divergence is compensated by the response filter and by the baseline filter  $M^2(\mathbf{f}) = [2\sin(\pi B f_x)]^2$ . However, the initial part of this filter proportional to  $f^4$  must be resolved by the numerical grid which has a sampling  $\Delta f = 1/L = 1/(DK_{size})$ . Even for  $B = 2D$ , the argument of the sine at the first grid point is  $\pi\Delta f B = \pi/8 \approx 0.39$ , hence the initial part of the integrand is sampled too crudely. To overcome the problem, the inner part of the response functions is re-sampled (blown-up) on a grid  $K_{blow}$  times finer. The choice  $K_{blow}K_{size} = 64$  ensures good sampling for moderate  $B/D$  ratios (the new frequency sampling is  $\Delta f = 1/(DK_{size}K_{blow})$  and the argument of the sine for  $B/D = 2$  becomes  $\pi/32$ ). However, a re-binning with simple linear interpolation does not work because it results in a linear behavior of the filter near the coordinate origin, hence gross over-estimate of the integral. Instead, the function  $|\tilde{F}(f)|^2/f^2$  is interpolated (it is nearly constant at  $f = 0$ ) and the result is then multiplied back by  $f^2$ . The correctness of the calculation has been checked by the stability of the result to the changes of  $K_{size}$  and  $K_{blow}$  by factors of two and also by doubling the number of grid points. Considering all approximations, the accuracy of the calculated  $K$  is estimated as  $\sim 3\%$ . The corresponding absolute error of  $r_0$  is 0.6 times less, or 1.8%.

In the present code, we apply the same aberration to both DIMM apertures. Only the circular mask  $W_0$  is implemented. These restrictions can be easily lifted.

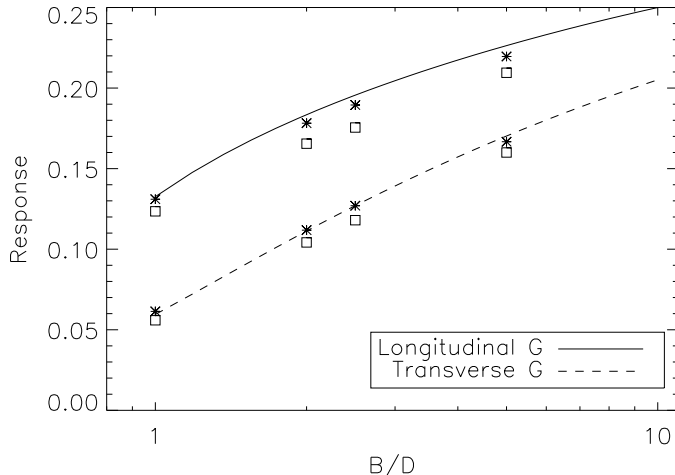


Figure 2: Response coefficients for longitudinal and transverse differential image motion, near field. Lines – ideal response for G-tilt, Eq. 11. Asterisks – analytical calculation, squares – simulation, both with  $\delta = 5$ .

Considering the complexity of the problem, a validation of response calculations by direct numerical simulation is required. The code `simatm.pro` simulates the distribution of the complex light amplitude after propagation through one or two turbulent layers. Then the code `simdim.pro` uses these “screens” to simulate the spots in a DIMM, possibly with some aberrations. All calculations

Table 1: Response coefficients  $K_l, K_t$  (in 1E-3) in presence of aberrations for a layer at  $z = 10$  km: analytic vs. simulation. The number of simulated Zernike aberrations  $N_Z$  and their amplitudes are given in the Noll’s notation. Parameters:  $B/D = 2.5$ ,  $\delta = 5$ .

$N_Z$	Ampl. rad	Simulated		Analytic	
		$K_l$	$K_t$	$K_l$	$K_t$
-	0	161	93	176	114
4	0.5	134	80	145	92
4	1	206	165	230	179
4	1.5	383	355	404	361
6	1	145	294	174	348
4,6	1,1	433	71	517	91
4,6	+0.7,0.7	255	73	295	94
4,6	-0.7,0.7	128	226	156	246

are monochromatic ( $\lambda = 0.5 \mu\text{m}$ ). Like any numerical simulator, `simdim` involves certain approximations and compromise choices, hence its results are not to be taken as absolute truth. The number of simulated quasi-independent realizations varied from 1000 to 10 000, hence the statistical error alone is 1-3%.

We simulated single phase screens with  $r_0 = 0.4$  m (seeing  $0.25''$ ), to ensure the small-signal regime. The screen was placed either at the ground (near-field) or at  $z = 10$  km. In the latter case, the scintillation index in 10-cm DIMM apertures is  $\sigma_I^2 = 0.0159$ . For both analytic and numerical cases, we adopted common parameters  $D = 0.1$  m,  $B = 0.25$  m,  $\delta = 5$ , unless indicated otherwise. The simulated pixel scale was  $0.161''$ .

Figure 2 compares the dependence of ideal (G-tilt), analytic and simulated response coefficients on the relative baseline  $B/D$ . Some difference between analytics and pure G-tilts is expected, but we see that the actual differences are within the stated 3% accuracy of the analytical calculation. The simulated response coefficients are systematically less than the analytic ones, by up to 10%.

Table 1 compares the analytic and simulated response coefficients in presence of aberrations and for a 10-km propagation. Considering all errors involved, the agreement is satisfactory. Hence, the analytic results can be trusted.

## 6 Stability of the DIMM response

In this Section, we use the analytic tool to study the stability of the DIMM response. In theory and current practice, it is always assumed that DIMM measures turbulence with a well-defined (theoretical) response coefficient independently of the location of turbulent layers and small instrument defects. In reality, the response is, of course, not constant.

The influence of the size of the centroid window  $\delta$  and aberrations on the longitudinal and transverse response coefficients is studied in Fig. 3. For perfect images without aberrations, the response is practically independent on  $\delta$  and is only slightly affected by the propagation (diminishes).

Aberrations of  $Z = 1$  rad amplitude correspond to the Strehl ratio  $e^{-Z^2} \approx 0.37$  – a slightly

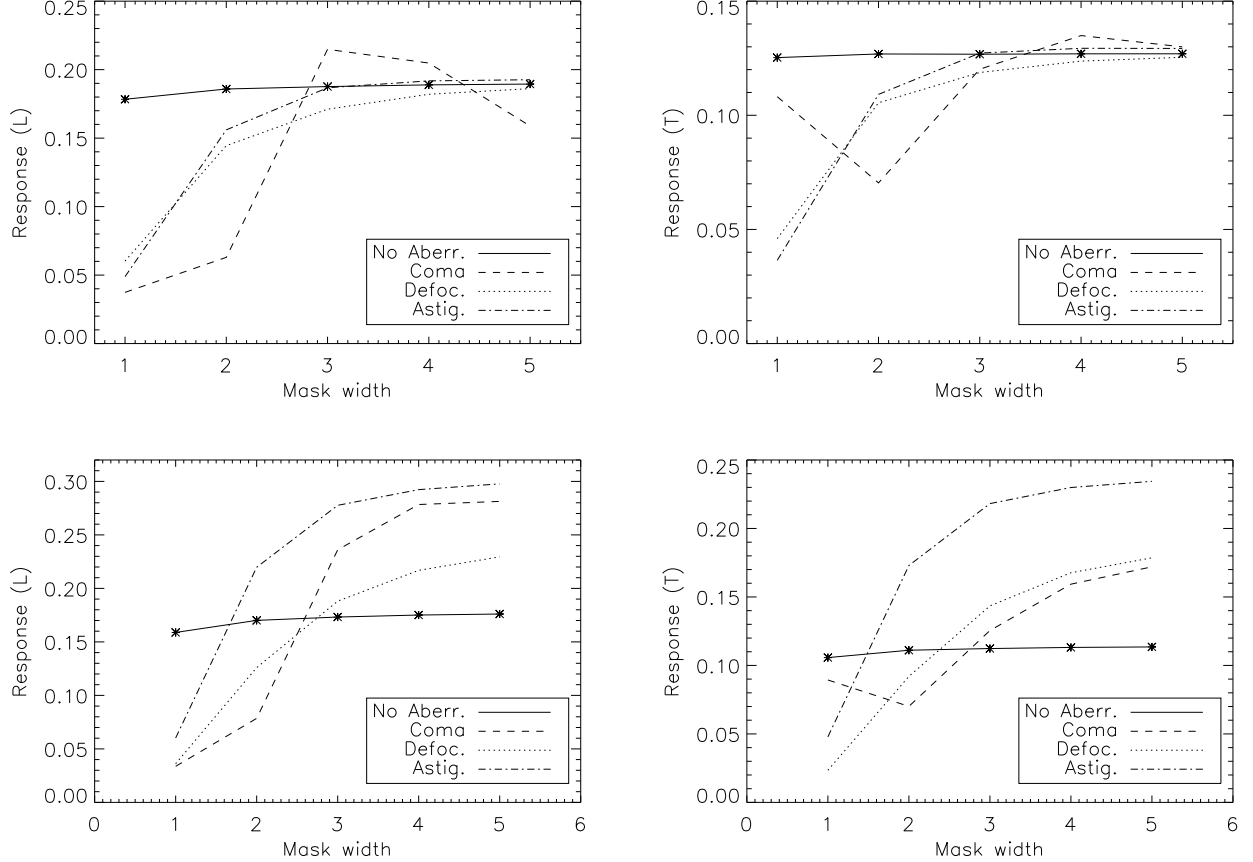


Figure 3: Response coefficients  $K_l$  (left) and  $K_t$  (right) as a function of the window width  $\delta$  for near field (top) and 10 km propagation (bottom). The amplitudes of the aberrations (coma  $Z_8$ , defocus  $Z_4$  and astigmatism  $Z_5$ ) are 1 radian. Parameters:  $D = 0.1$  m,  $B = 0.25$  m.

distorted, but still quite marked diffraction spot. In the near field, the aberrations, generally, reduce the response, but this reduction is small if the centroiding window is sufficiently large, e.g.  $\delta = 5$ . The case of coma is an exception. A tilt of 1 rad was applied in combination with coma, to preserve roughly the center of the spot with respect to the mask. The amount of this tilt (or, equivalently, the method to pre-center the spot before calculating the final signal) is important and influences the response.

The effect of the 1-radian aberrations for a 10-km layer is dramatic and leads to a strong over-estimation of turbulence for large centroid windows. Thus, the “weighting function” of DIMM – the dependence of its response on the propagation distance – is not constant. For a perfect instrument, it slightly declines with  $z$ , but even a small amount of aberration is sufficient to get the response strongly rising with altitude.

The dependence of the response on the defocus amplitude is plotted in Fig. 4. Alarmingly, even a small defocus, with a large window  $\delta = 5$ , influences the response coefficients for the 10-km layer.

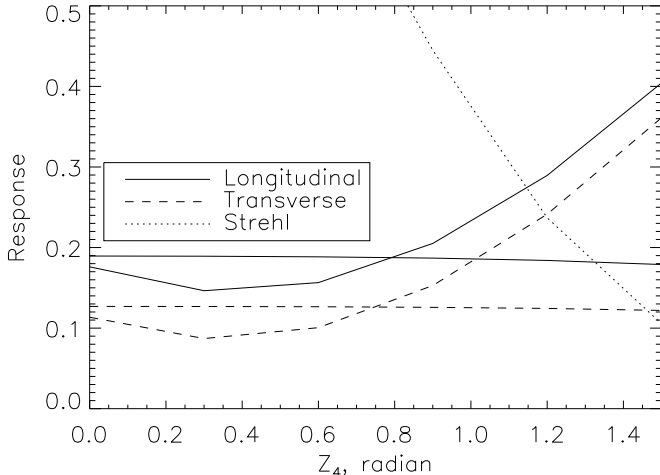


Figure 4: Response coefficients for near-field (nearly constant curves) and 10-km layer (growing curves) as a function of the defocus amplitude. Parameters:  $D = 0.1$  m,  $B = 0.25$  m,  $\delta = 5$ .

These coefficients decrease at first, then increase for a larger defocus. The decrease of the high-altitude response for a small defocus is confirmed by the simulations (Table 1, line 2). At defocus of 1 rad, the spot has still a central peak with increased “wings” (Fig. 5). The signal becomes influenced by the amplitude gradient in the x-direction, as expected. At 1.5 rad, a minimum at the spot center appears and the sensitivity to scintillation increases even more.

It is instructive to consider a combination of defocus with astigmatism  $Z_6$  (last 2 lines in Table 1). With both aberrations positive, the image is distorted into a horizontal “line”. Consequently, the longitudinal coefficient is influenced by the scintillation. With the opposite signs, the image is vertical and the transversal coefficient is affected instead.

## 7 Conclusions

The standard theory of DIMM has been developed for near-field (pure phase) distortions and ideal centroids. Here we show that the response coefficients for centroiding in a wide window closely match their theoretical values for G-tilt and are only weakly affected by the window size and small aberrations.

On the other hand, the DIMM response to high turbulence is shown to be extremely sensitive to aberrations. Small aberrations decrease the response, large aberrations increase it. The variations are quite significant ( $\sim 20\%$ ) even for aberrations below 1 radian (Strehls above 0.37). DIMM can either “over-shoot” or “under-shot”. For example, a defocus of only 0.3 rad (24 nm rms wavefront aberration, Strehl 0.91) reduces the longitudinal and transverse response to a 10-km layer by 0.77 and 0.69, respectively. The bias on seeing will be 0.86 and 0.80. To our knowledge, no DIMM instrument is controlled optically to that level of accuracy. Hence, when high turbulence dominates, DIMM can be easily biased both ways by 20% or more.

## References

- [1] R. Noll, “Zernike polynomials and atmospheric turbulence”, *J. Opt. Soc. Am.*, **66**, 207-211 (1976)



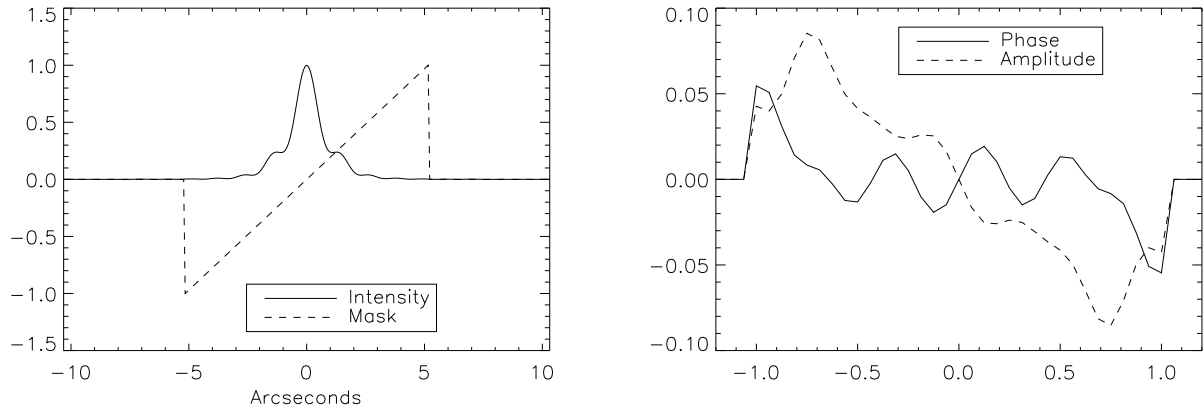


Figure 5: Image and mask profiles (left) and the response functions (right) for a defocus of 1 radian. Compare with Fig. 1. Parameters:  $D = 0.1$  m,  $B = 0.25$  m,  $\delta = 5$ .

- [2] F. Roddier, “The effects of atmospheric turbulence in optical astronomy”, in Progress in Optics, **19**, 281-376 (1981)
- [3] A. Tokovinin, “From differential image motion to seeing”. PASP, 114, 1156 (2002).